

ALMA MATER STUDIORUM
UNIVERSITY OF BOLOGNA

Structural and Environmental Health Monitoring and Management (SEHM2)
Department of Electrical, Electronic, and Information Engineering
"Guglielmo Marconi" (DEI)

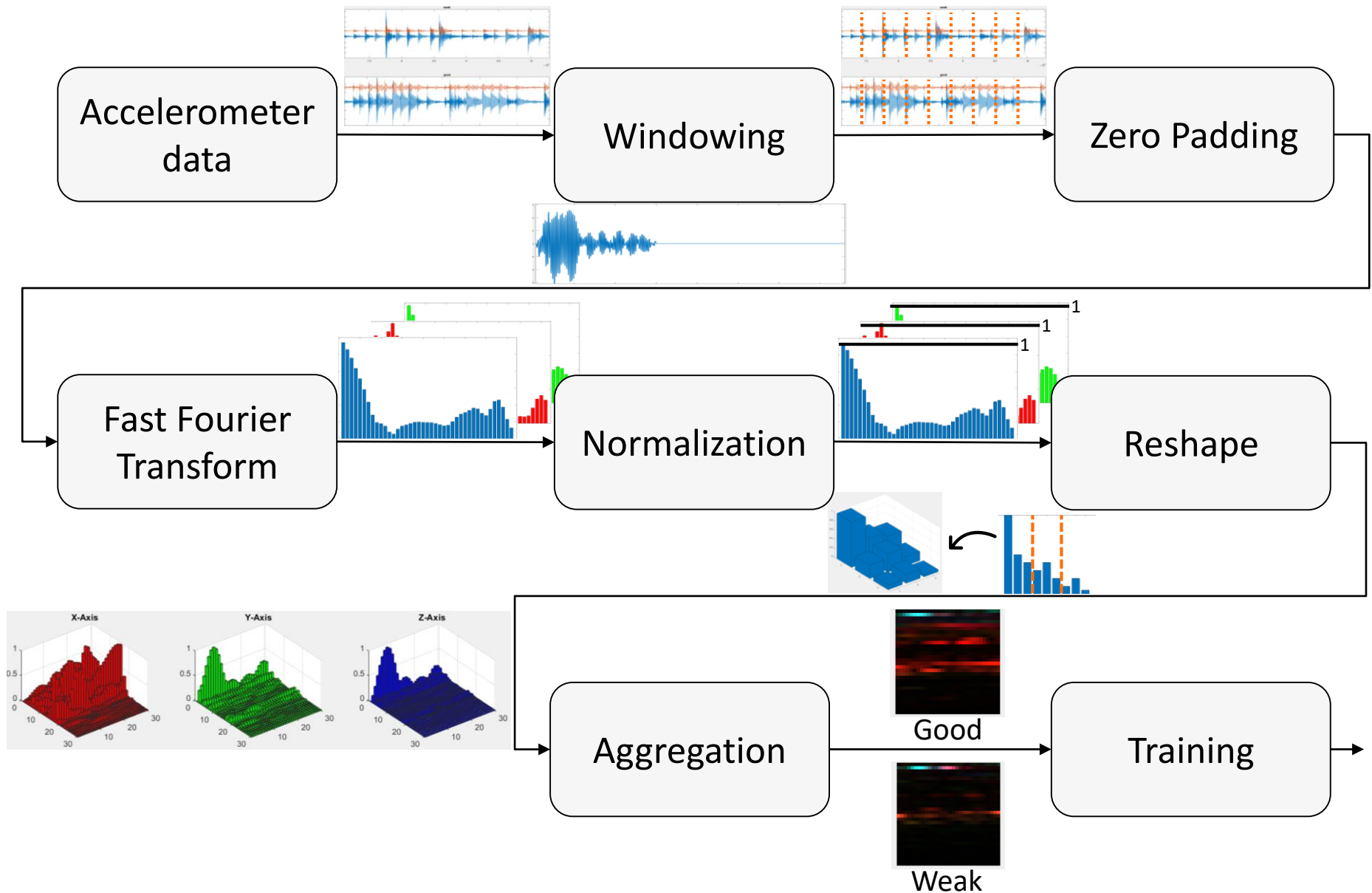
Machine Learning for Structural Classification and Monitoring (2nd Year)

ELIA FAVARELLI

Table of contents

- ❖ Last year
 - Proposed strategy
 - Results and problems
- ❖ Timeline
- ❖ **Z-24** Bridge
 - Structure description
 - Monitoring phases
- ❖ Operational modal analysis (**OMA**)
 - Models overview
 - Output-only models
 - Stochastic subspace identification (**SSI**)
 - Stabilization diagram
- ❖ Mode selection techniques
 - Modal assurance criterion (**MAC**)
 - Mean phase deviation (**MPD**)
 - Dumping ratio check
 - Complex conjugate poles check
- ❖ Clustering
- ❖ Tracking
 - Algorithm
 - Features distribution
- ❖ Anomaly detection algorithms
 - Principal component analysis (**PCA**)
 - Kernel principal component analysis (**KPCA**)
 - Gaussian mixture model (**GMM**)
 - Autoassociative neural network (**ANN**)
 - One class classifier neural network (**OCCNN**)
 - Comparison
- ❖ Conference papers
 - Anomaly detection on **Z-24**
 - Anomaly detection for intrusion detection
 - Topology inference
- ❖ Future works...

Last year...: Proposed strategy



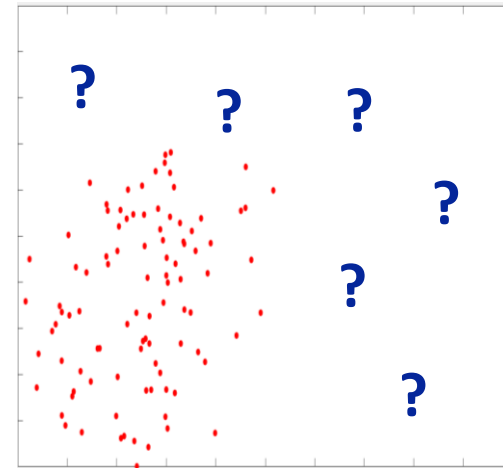
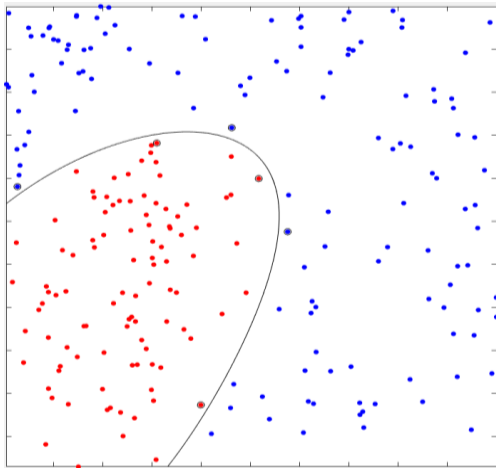
Last year: Results and problems

Results:

- ❖ Accuracy = 95%
- ❖ Missed detection = 5%
- ❖ False alarm = 5%

Main Problems:

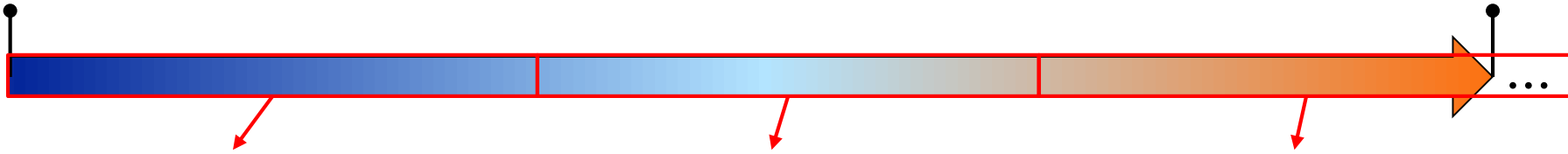
- ❖ It is often **impossible** to have training data of **weak** conditions in real scenarios
- ❖ It is **impossible** to train **Convolutional Neural Networks** with **only one class**
- ❖ Comparison with literature



Timeline

November 2018

November 2019



Review of the state-of-art in structural monitoring and anomaly detection:

- ❖ Operational modal analysis (**OMA**)
- ❖ Output-only modal identification
- ❖ Auto-regressive moving average vector models (**ARMA models**)
- ❖ Stochastic subspace identification (**SSI**)
- ❖ Principal component analysis (**PCA**)
- ❖ Kernel PCA (**KPCA**)
- ❖ Gaussian mixture model (**GMM**)
- ❖ Autoassociative neural network (**ANN**)

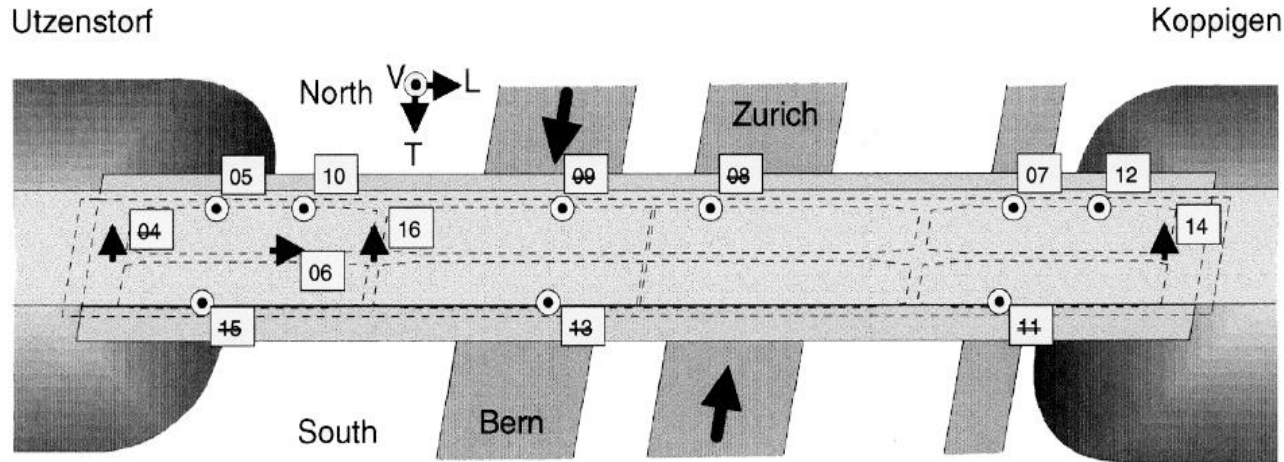
Investigation of structures widely known in literature and access to databases:

- ❖ **Z-24 bridge**
- ❖ Sensors displacement
- ❖ Structure characteristics
- ❖ Monitoring period
- ❖ Monitoring characteristics
- ❖ Temperature effects
- ❖ Damage condition
- ❖ Database management
- ❖ Accelerometer data
- ❖ Environment data
- ❖ **Down sampling**
- ❖ **Decimation**
- ❖ Filtering

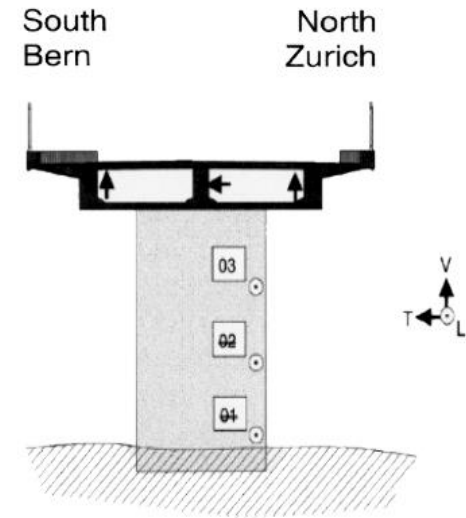
Implementation of novel techniques for anomaly detection in SHM and ...:

- ❖ One class classifier neural network (**OCCNN**)
- ❖ Automated anomaly detection in **SHM**
- ❖ Anomaly detection for intrusion detection
- ❖ **Machine learning** algorithms for topology inference
- ...
- ❖ Sensor **failure** effects
- ❖ Quantization effects
- ❖ Sensor failure detection

Z-24 bridge: structure description



Cross view



- ❖ Classical post-tensioned concrete two-cell box girder bridge with a main span of 30m and two side spans of 14m
- ❖ **Long term monitoring** in standard condition for 1 year
- ❖ **Short term monitoring** in progressive damage condition
- ❖ **15 accelerometers** equipped
- ❖ **9 failures** during the monitoring period
- ❖ **8 reliable** sensors used for the following processing

Z-24 bridge: Monitoring phases

4 August	Undamaged condition
9 August	Installation of pier settlement system
10 August	Lowering of pier, 20 mm
12 August	Lowering of pier, 40 mm
17 August	Lowering of pier, 80 mm
18 August	Lowering of pier, 95 mm
19 August	Lifting of pier, tilt of foundation
20 August	New reference condition
25 August	Spalling of concrete at soffit, 12 m ²
26 August	Spalling of concrete at soffit, 24 m ²
27 August	Landslide of 1 m at abutment
31 August	Failure of concrete hinge
2 September	Failure of 2 anchor heads
3 September	Failure of 4 anchor heads
7 September	Rupture of 2 out of 16 tendons
8 September	Rupture of 4 out of 16 tendons
9 September	Rupture of 6 out of 16 tendons

Nomenclature

- f_s = sample frequency [Hz]
- T_a = acquisition time [s]
- N_s = number of samples
- N_a = number of acquisitions

LONG TERM MONITORING

❖ For 1 year each hour an acquisition is taken from all the sensors:

- $f_s = 100$ Hz
- $T_a = 655.36$ s
- $N_s = 65536$

SHORT TERM MONITORING

❖ On the left the progressive damage generated artificially by a lowering system

* Unfortunately around 44% of the data have been lost

- $N_a = 4107$

Finite element method

Pros:

- **Accurate** estimation of modal parameters

Cons:

- Computationally **complex**
- Need an accurate knowledge of the structure
- **Not generalizable**

Peak Picking

Pros:

- **Low complexity**
- **Blind** method

Cons:

- **Low accuracy** in the modal parameter estimation
- **Input sensitive**

ARMA method

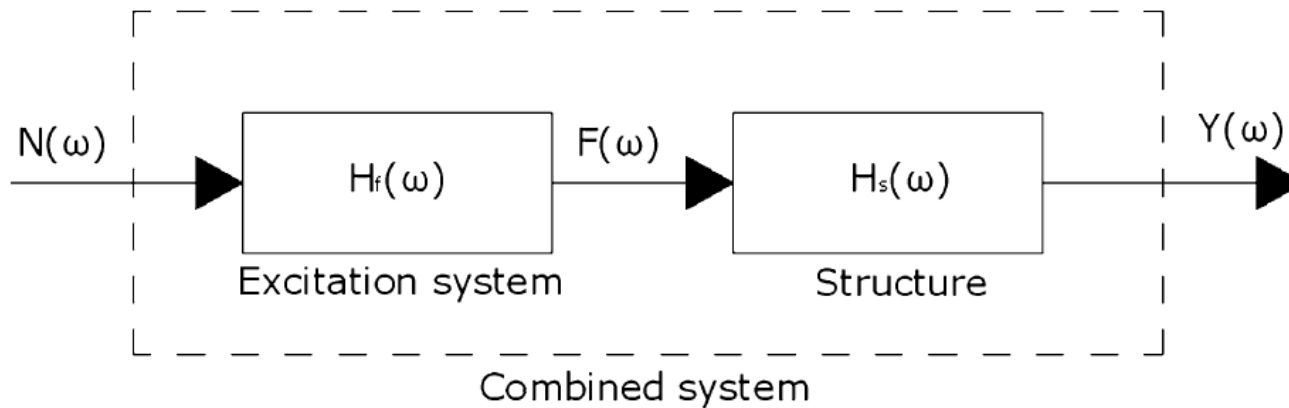
Pros:

- No need of accurate knowledge of the structure
- **Generalizable**

Cons:

- Computationally **complex**
- **Convergence** problems

OMA: Output-only models



Nomenclature

- $N(\omega)$ = Input excitation
- $H_f(\omega)$ = Excitation system transfer function
- $F(\omega)$ = Excitation system output
- **$H_s(\omega)$ = Structure transfer function**
- $Y(\omega)$ = Structure output

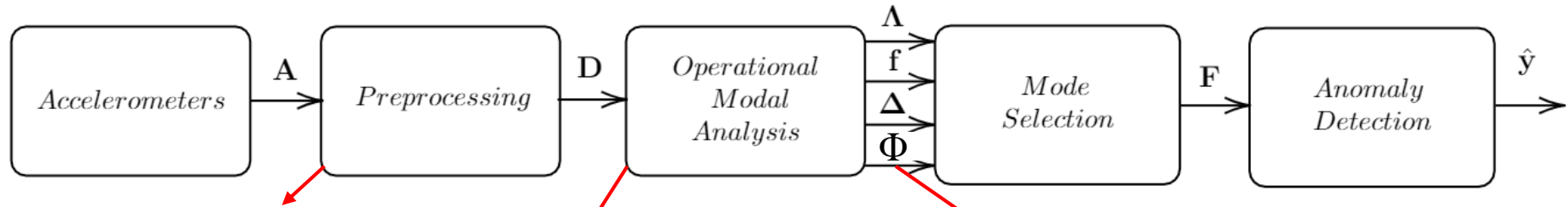
Hypothesis

- $n(t)$ = white noise $\rightarrow N(\omega) = \text{Flat}$
- **$H_f(\omega) = \text{broadband}$**
- **$H_s(\omega) = \text{narrowband}$**

Result

- $F(\omega)$ excite all the modes of **$H_s(\omega)$**

OMA: Stochastic subspace identification (SSI)



Preprocessing

- **Filtering**
- **Decimation**

SSI method

Pros:

- No need of an accurate knowledge about the structure
- No need of a structure simulation (blind method)
- **Output-only** model
- Closed form solution
- Good **accuracy** in the modal parameter estimation

Cons:

- Computationally **complex**

Model parameters (input)

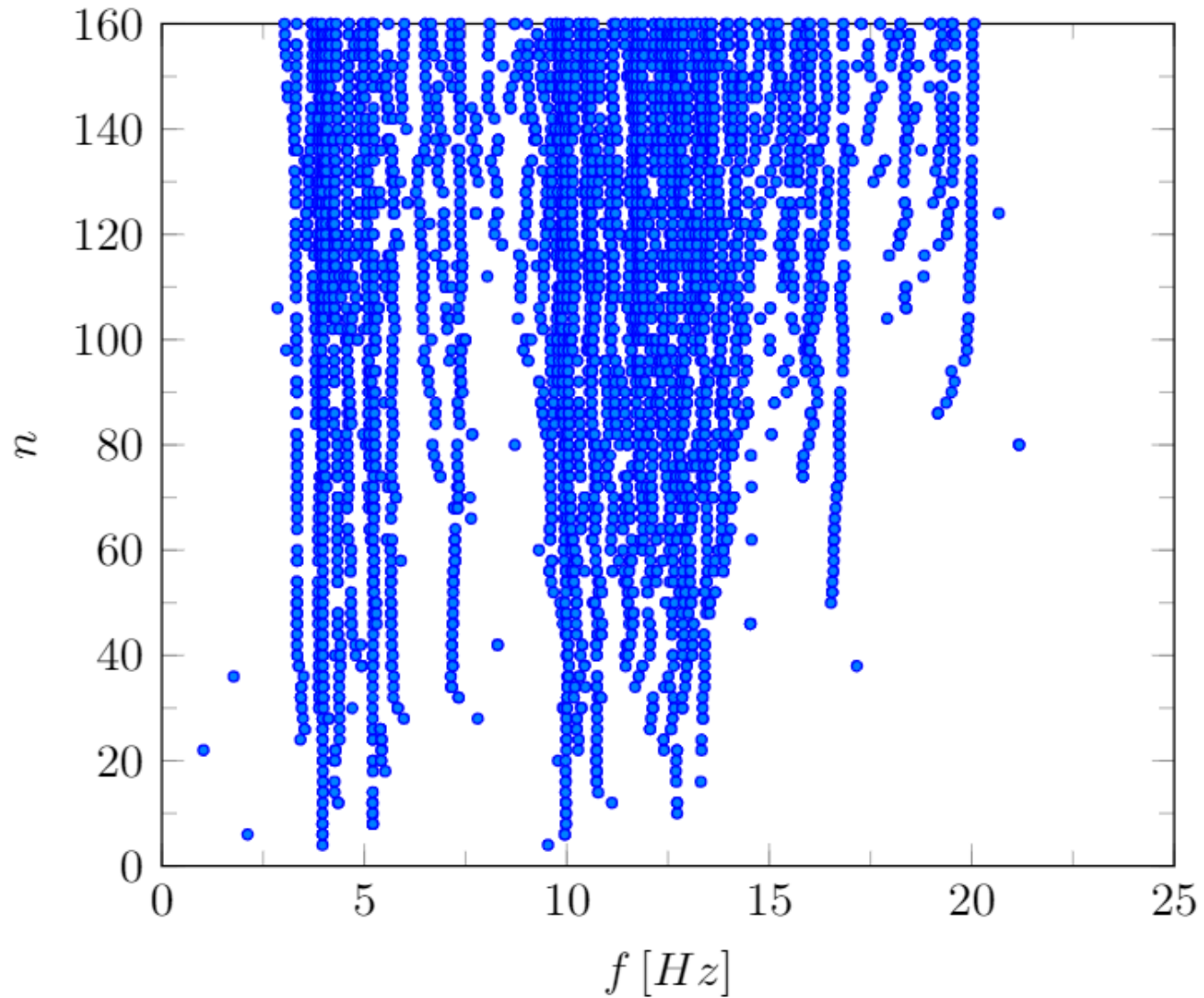
- n = model order
- i = time lag
- l = number of sensors

Modal parameters (output)

- f = Natural frequencies (scalar)
- Λ = Eigenvalues (vector)
- Δ = Damping ratios (scalar)
- Φ = Mode shapes (matrix)

*parameters extracted for each measurement (each hour)

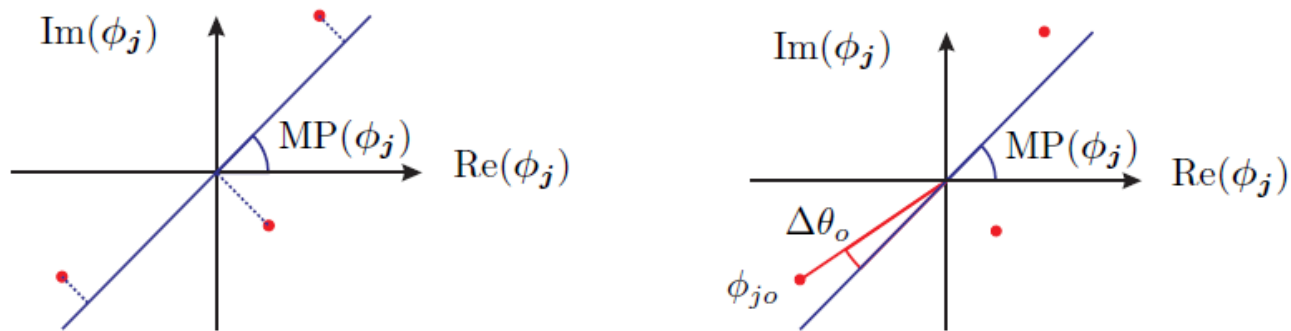
OMA: Stabilization diagram



$$MAC(\Phi^{(j)}, \Phi^{(l)}) = \frac{|\Phi^{(j)*} \Phi^{(l)}|}{\|\Phi^{(j)}\|_2 \|\Phi^{(l)}\|_2}$$

- Dimensionless **correlation** coefficient between mode shapes
- Takes value between **0** and **1**, values larger than **0.9** indicate consistent correspondence and probably **physical** modes

Mode selection techniques: MPD



- Indicator of the mode shape components deviation with respect to the mean phase (**MP**)
- Singular value decomposition (**SVD**): $USV^T = [\text{Re}\{\Phi^{(j)}\} \quad \text{Im}\{\Phi^{(j)}\}]$
- $U \in \mathbb{R}^{2 \times 2}$, $S \in \mathbb{R}^{2 \times 2}$ and $V \in \mathbb{R}^{2 \times 2}$

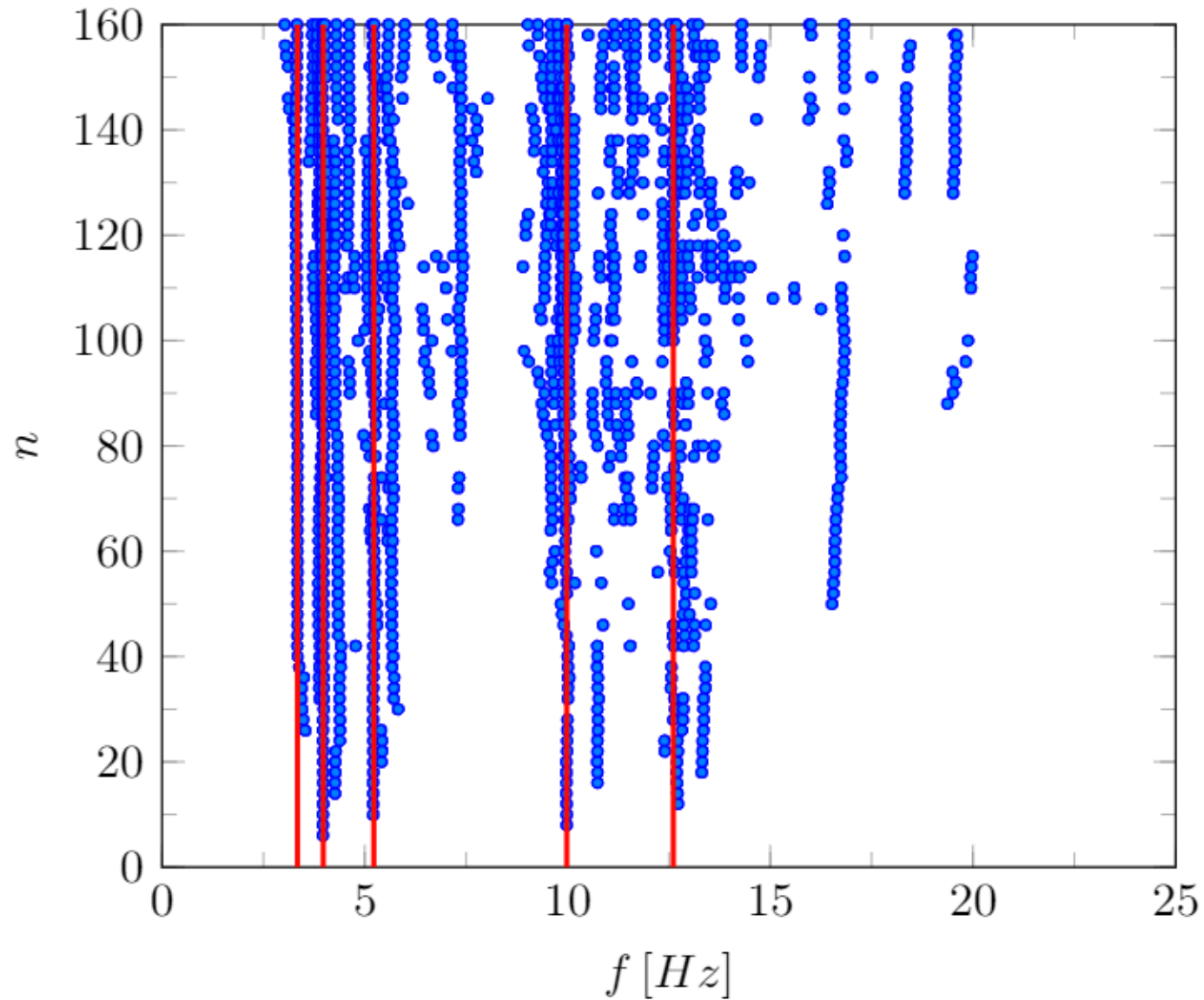
$$MP(\Phi_j) = \arctan \left(\frac{-V_{12}}{V_{22}} \right)$$

$$MPD(\Phi_j) = \frac{\sum_{k=1}^{n_y} |\Phi_{jk}| \arccos \left| \frac{\text{Re}\{\Phi_{jk}\} V_{22} - \text{Im}\{\Phi_{jk}\} V_{12}}{\sqrt{V_{12}^2 + V_{22}^2} |\Phi_{jk}|} \right|}{\sum_{k=1}^{n_y} \Phi_{jk}}$$

- When $\frac{MPD(\Phi_j)}{90^\circ} < \mathbf{0.75}$ the mode is considered **spurious**

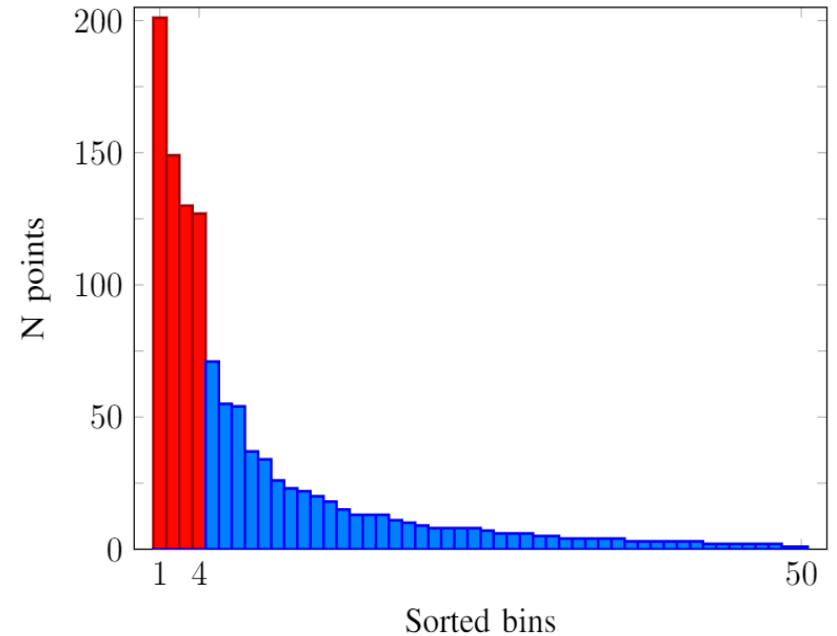
- **Damping ratios check:** for each mode we have a dumping ratio $\delta(j)$, in real structures this factor must be positive and lower than **0.2** (otherwise the structure will be unstable) hence only modes with **$0 < \delta(j) < 0.2$** are considered
- **Complex conjugate poles check:** if the eigenvalues of a mode do not have a complex conjugate probably represent a spurious mode and will be deleted, moreover if **$\text{Re}\{\lambda(j)\} > 0$** the mode represent an unstable structure hence the relative mode will be considered as spurious

Cleaning & Clustering



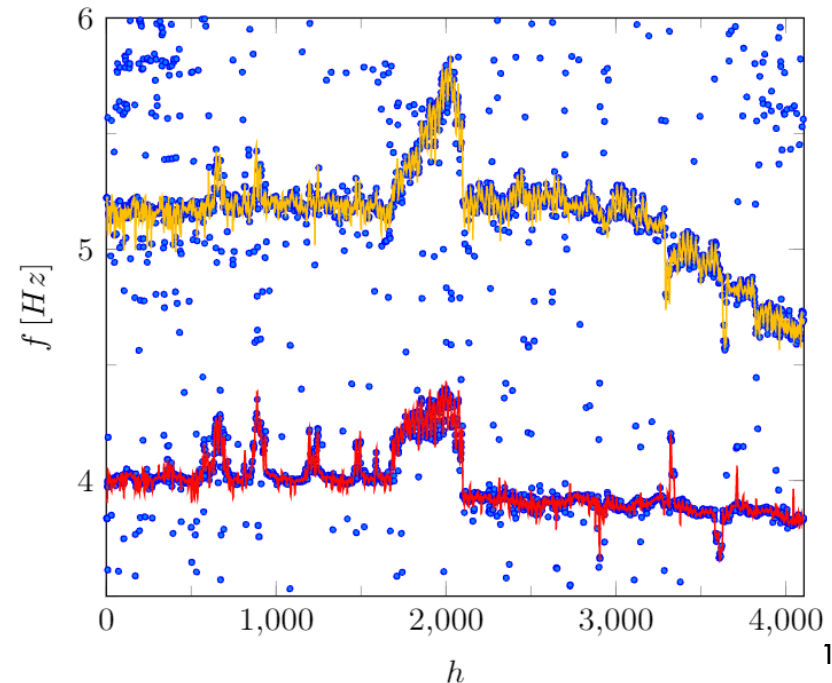
❖ Starting phase:

- **200 h** of measurements
- Rectangular window, size=**0.2 Hz**, without overlap, range **[0, 10Hz]**
- Select the **more relevant** components as starting points

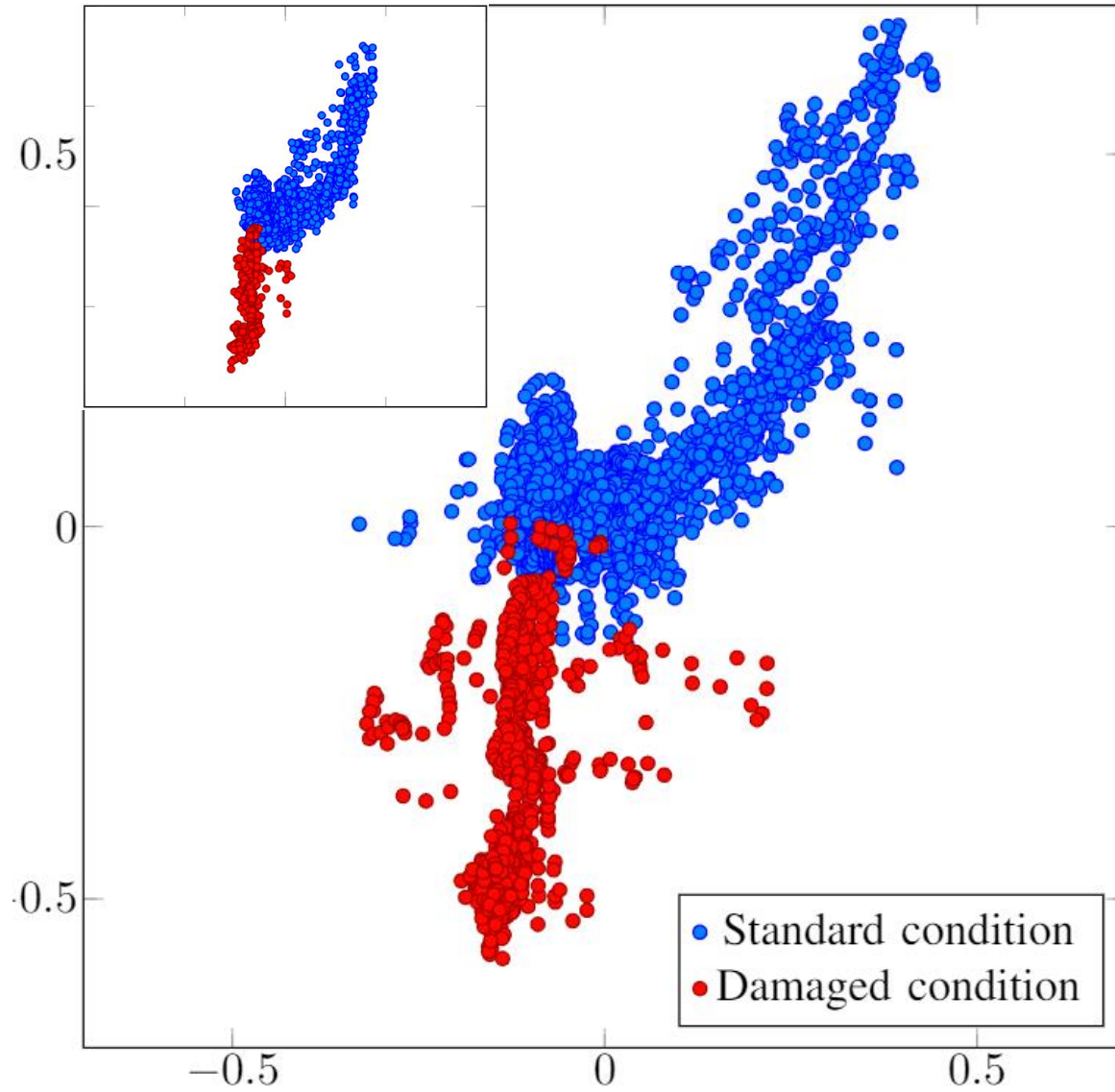


❖ Online phase:

- **n** = iteration number
- **3 h** of measurements
- Gaussian window, **$\sigma=0.16$** , **μ_n** = mean of the elements that fall in the interval **$[\mu_{n-1} \pm 2\sigma]$**
- **μ_0** = Starting points



Tracking: Features Distribution



Anomaly detection algorithms: PCA

- **Covariance matrix** evaluation

$$\Sigma = \frac{\mathbf{X}^T \mathbf{X}}{N_X - 1}$$

- **Eigenvalues** decomposition

$$\Sigma = \mathbf{V} \Lambda \mathbf{V}^T$$

- Projection in a **lower dimensional** feature space

$$\mathbf{V}_P = [\mathbf{v}_1 | \mathbf{v}_2 | \dots | \mathbf{v}_P]$$

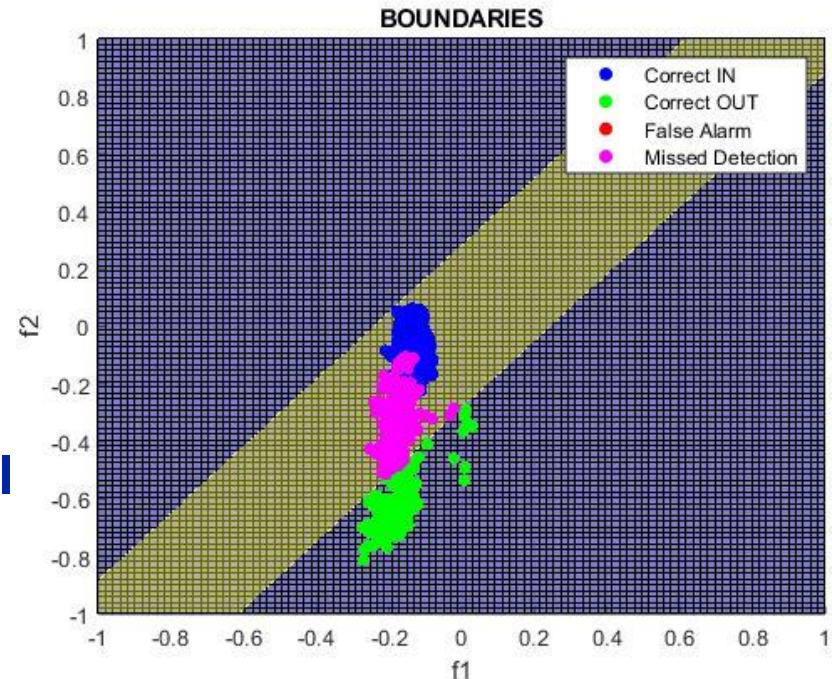
$$\mathbf{X}_P = \mathbf{X} \mathbf{V}_P$$

- **Reconstruction**

$$\tilde{\mathbf{X}} = \mathbf{X}_P \mathbf{V}_P^T$$

- **Error** evaluation (Euclidean distance)

$$e_{x_n} = \sqrt{\sum_{d=1}^D (x_{n,d} - \tilde{x}_{n,d})^2}$$



Confusion Matrix

	0	1	
0	218 26.9%	0 0.0%	100% 0.0%
1	244 30.2%	347 42.9%	58.7% 41.3%
	47.2% 52.8%	100% 0.0%	69.8% 30.2%
	0	1	Target Class

Anomaly detection algorithms: KPCA

- **Remapping** of the points in a new feature space (**RBF**)

$$K_n^{(z)} = e^{-\gamma \|z - x_n\|^2} \quad \text{with} \quad n = 1, 2, \dots, N_X$$

- Application of the **PCA** algorithm to the new points
- **Error** evaluation (Euclidean distance)

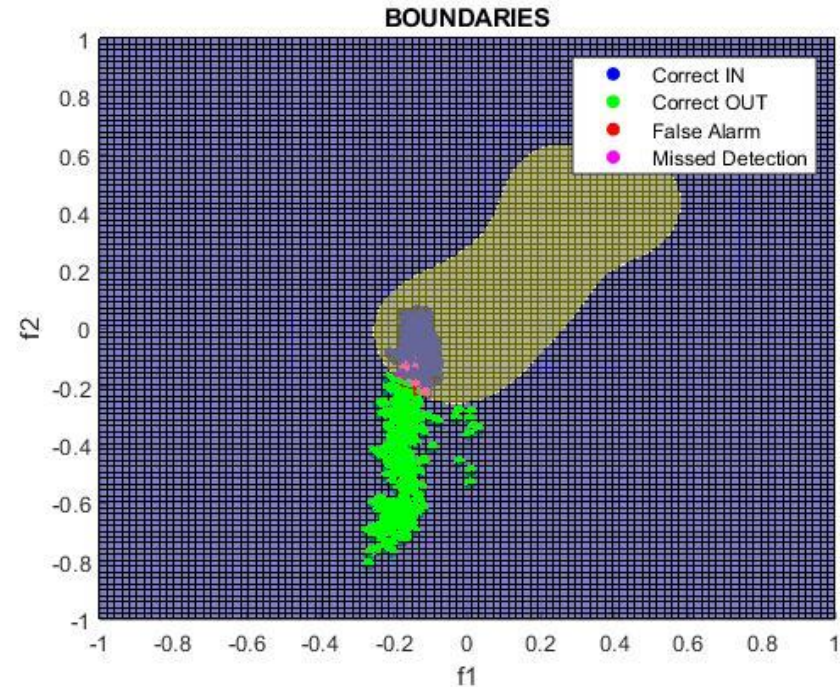
$$e_{x_n} = \sqrt{\sum_{d=1}^D (x_{n,d} - \tilde{x}_{n,d})^2}$$

where

$$D = N_X$$

$$X_n = K_n$$

$$\tilde{x}_n = \tilde{K}_n$$

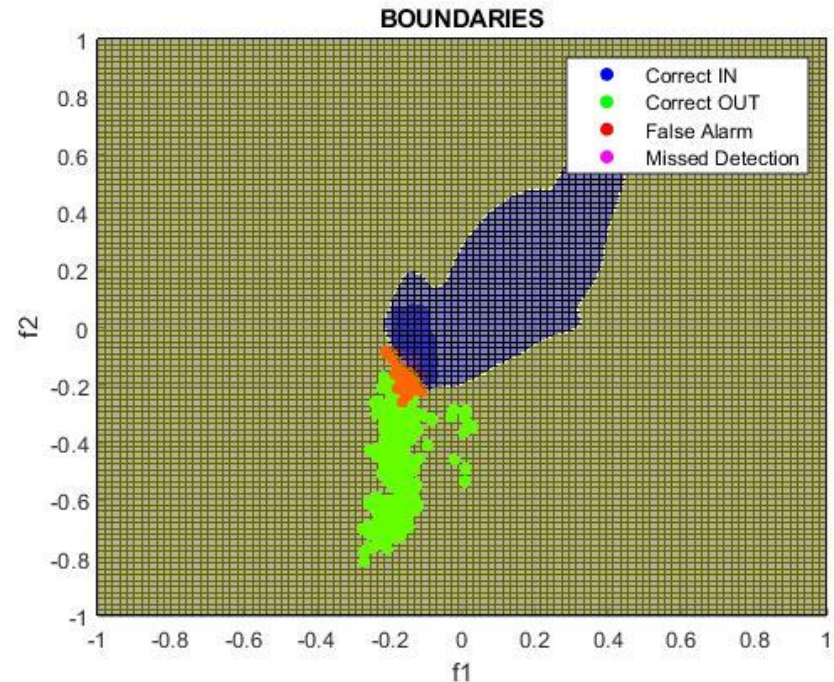


Confusion Matrix

	0	1	
0	440 54.4%	6 0.7%	98.7% 1.3%
1	22 2.7%	341 42.2%	93.9% 6.1%
	95.2% 4.8%	98.3% 1.7%	96.5% 3.5%
	0	1	Target Class

Anomaly detection algorithms: GMM

- Model order selection
 $M = 10$
- Random initialization of M Gaussian functions with covariance matrix Σ_m and mean value μ_m
- Parameter **optimization** (stochastic gradient descent) to best fit the data distribution
- **Threshold** setting to ensure a false alarm in the training set equal to **0.01**



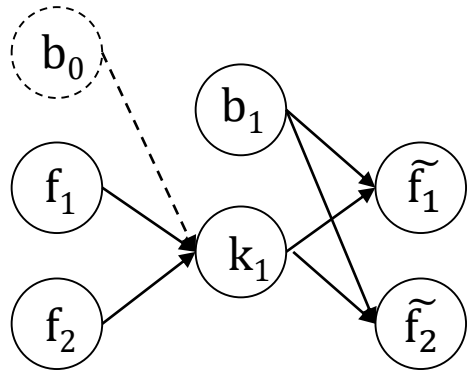
Confusion Matrix

	0	1	
0	460 56.9%	83 10.3%	84.7% 15.3%
1	2 0.2%	264 32.6%	99.2% 0.8%
	0	1	89.5% 10.5%

Output Class

Target Class

Anomaly detection algorithms: ANN

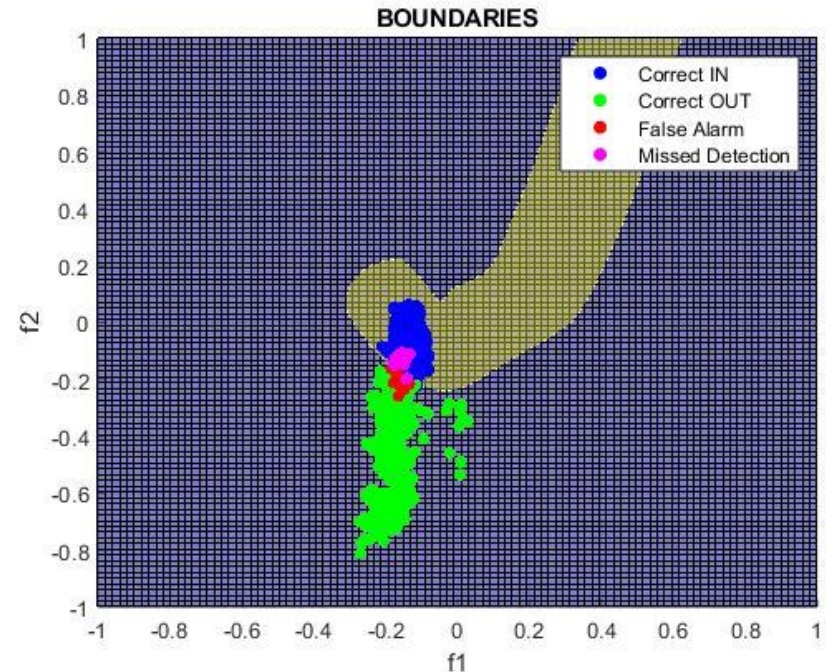


- **Mapping** in a low dimensional feature space (bottleneck)

$$f_1, f_2 \rightarrow k_1$$

- **Remapping** in the starting feature space minimizing the reconstruction error

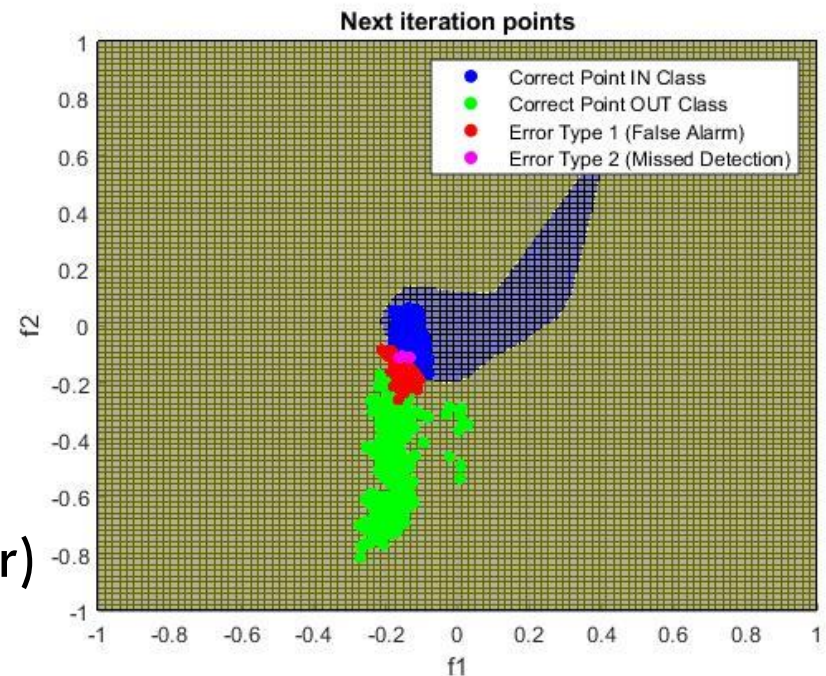
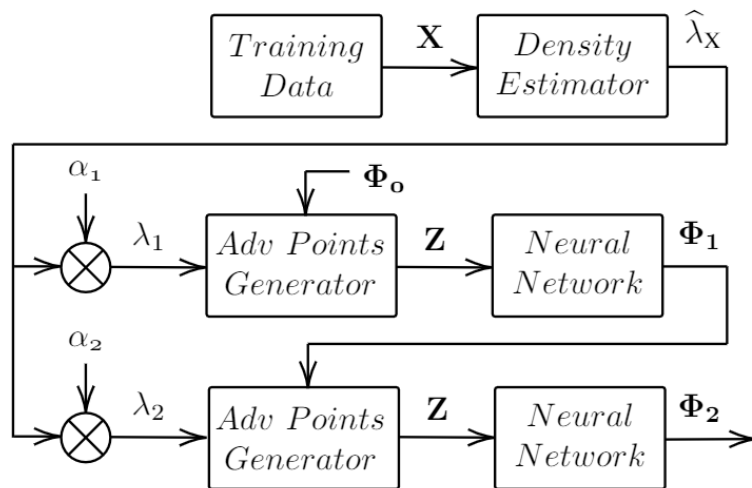
$$k_1 \rightarrow \tilde{f}_1, \tilde{f}_2$$



Confusion Matrix

	0	1	
0	437 54.0%	7 0.9%	98.4% 1.6%
1	25 3.1%	340 42.0%	93.2% 6.8%
	94.6% 5.4%	98.0% 2.0%	96.0% 4.0%
	0	1	Target Class

Anomaly detection algorithms: OCCNN



- Density estimator (**Pollard's estimator**)

$$\hat{\lambda}_X = \frac{\left(\sum_{n=1}^{N_p} k_n\right) - 1}{\pi \sum_{n=1}^{N_p} r_n^2}$$

$\hat{\lambda}_x$ = estimated density, $N_p = n$ points,

k_n = k_n -th neighbor,

r_n = distance from the k_n -th neighbor

- Hyper parameters setting

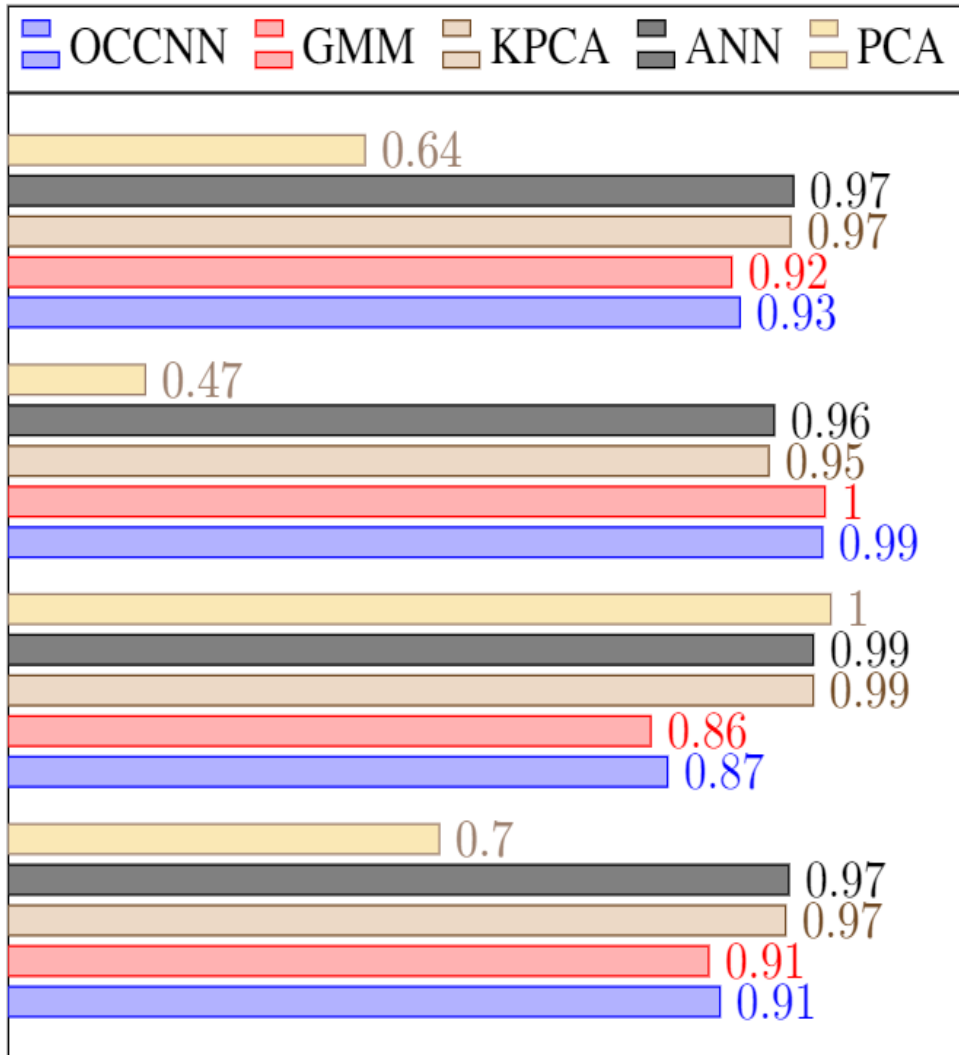
$$\alpha_1 = 0.3, \alpha_2 = 0.8$$

- **Feed-forward NN** with two hidden layers and **50 neurons** in each layer

Confusion Matrix

	0	1	
0	459 56.7%	66 8.2%	87.4% 12.6%
1	3 0.4%	281 34.7%	98.9% 1.1%
	99.4% 0.6%	81.0% 19.0%	91.5% 8.5%
	0	1	Target Class

Anomaly detection algorithms: Comparison



PREDICTIVE VALUES

POSITIVE (1) NEGATIVE (0)

ACTUAL VALUES

POSITIVE (1)	TP	FN
NEGATIVE (0)	FP	TN

❖ **Accuracy:**

$$Acc = \frac{TP+TN}{TP+TN+FP+FN}$$

❖ **Precision:**

$$Prec = \frac{TP}{TP+FP} = \frac{TP}{PP}$$

❖ **Recall or Sensitivity:**

$$Rec = \frac{TP}{TP+FN} = \frac{TP}{P}$$

❖ **F1 score:**

$$F1 = 2 * \frac{Prec*Rec}{Prec+Rec}$$

One Class Classifier Neural Network for Anomaly Detection in Low Dimensional Feature Spaces

Elia Favarelli, Enrico Testi, and Andrea Giorgetti
DEI, University of Bologna
Via dell'Università 50, 47522 Cesena, Italy
e-mail: {elia.favarelli, enrico.testi4, andrea.giorgetti}@unibo.it

Abstract—In the last decade, many approaches have been developed to solve one-class classification (OCC) problems for anomaly detection. Many of them rely on estimating the statistical distribution of the data, find hidden patterns, or remap the data in advantageous feature spaces. This kind of techniques usually needs some a priori knowledge of the data distribution (i.e., Gaussian) or the setting of some parameters to achieve good classification performance, making their use less effective when the data distribution is unknown. In this paper, we propose a novel blind anomaly detection for low dimensional feature spaces, that exploits the flexibility of the neural network (NN) structure to find the class boundaries without any information about the shape of the data distribution. To prove the generality of the solution, we tested many different class shapes, and we applied it to a structural health monitoring (SHM) case study. Without requiring the tuning of hyperparameters, the performance of the proposed algorithm overcomes that of some known approaches like principal component analysis (PCA), kernel principal component analysis (KPCA), Gaussian mixture model (GMM), and autoassociative neural network (ANN) in many cases, and performs well in the specific SHM setting.

I. INTRODUCTION

In the last decade, we have witnessed the rise of cyber-physical systems (CPSs) as the new era of interconnected objects. CPSs consist of sensors to monitor the physical environment and make decisions to affect physical processes through closed loop controls. These systems will be widely adopted in critical infrastructures, such as oil and natural gas distribution, electrical power grid, industrial automation, automotive, and medical devices [1]–[5]. Therefore, system parameter monitoring and behavior classification are becoming of paramount importance. Another fascinating application domain for CPSs will be structural health monitoring (SHM) for the timely detection of damage on a structure, its location, and type with application ranging from historical buildings to large infrastructures.

Depending on the domain of application an anomaly is called by alternative terms: alien class, abnormal class, outlier class, and attacker/intruder class. The target of anomaly detection is to discern unusual samples in data by learning a model that accurately describes normality. Generally, this is solved as an unsupervised learning problem where the training dataset consists of normal samples since the anomalous samples are not known a priori. This type of problem is also known as one-class classification (OCC) [6]–[9]. From this perspective,

when the normal class boundaries are non-linear, and the data distribution is unknown, a blind solution able to find complex patterns becomes really suggestive.

Nowadays, many different techniques are widely used to solve OCC problems [10]. In this paper, principal component analysis (PCA) [11], [12], kernel principal component analysis (KPCA) [13], Gaussian mixture model (GMM) [10], and autoassociative neural network (ANN) [14], will be presented as a benchmark. These techniques, while effective in some situations, present quite well known limitations:

- PCA: finds linear boundaries, so it is recommended only if the data are linearly separable in the feature space;
- KPCA: overcomes the PCA limitations by managing non-linear boundaries, but needs the choice of an appropriate kernel function;
- GMM: finds non-linear boundaries but assumes that the data can be described by a mixture of Gaussian distributions and needs the choice of the most appropriate model order;
- ANN: finds non-linear boundaries thanks to the non-linear activation functions present in the hidden layers but works better when the feature space dimensionality is high.

To overcome such limitations, we propose a neural network (NN)-based solution able to find non-linear boundaries without the need of hyperparameters. Our solution relies on density estimation of the training data distribution, the generation of an adversarial class to represent the possible anomalies, and finally, the training of a NN with the two classes. The same procedure is repeated twice to improve NN detection capability.

Throughout the paper, capital bold letters denote matrices, lowercase bold letters denote vectors, $(\cdot)^T$ stands for transposition, $\|\cdot\|$ is the ℓ_2 norm of a vector, \otimes stands for the Kronecker product, $\mathbf{1}_N$ is a column vector of all ones and size N , $\mathbb{E}\{\cdot\}$ is the expectation operator, and $\mathbb{V}\{\cdot\}$ is the variance operator. The rest of the paper is organized as follows. In Section II the data set and data normalisation are described. Section III provides an overview of existing OCC techniques. The one-class classifier neural network (OCCNN) is presented in Section IV. Numerical results and a case study are given in Section V and Section VI, respectively. Conclusions are drawn

- ❖ PCA
- ❖ KPCA
- ❖ GMM
- ❖ ANN
- ❖ OCCNN
- ❖ Stress test
- ❖ Hyperparameter setting
- ❖ Z-24 case of study
- ❖ Accuracy
- ❖ Precision
- ❖ Recall
- ❖ F1 score
- ❖ Algorithm comparison
- ❖ F1 > 93% with OCCNN

FUTURE EXTENSIONS

- ❖ High dimensional feature space
- ❖ New damage sensitive feature extraction

*accepted ICSPCS, Australia, December 2019

Conference papers: Anomaly detection for intrusion detection

- ❖ Beacon extraction
- ❖ WiFi standard
- ❖ Power spectrum density (**PSD**)
- ❖ Beacon average
- ❖ **PCA**
- ❖ **KPCA**
- ❖ Received signal strength (**RSS**) based algorithms
- ❖ Algorithm comparison
- ❖ **Acc > 95%** with only 1 beacon (**KPCA**) without signal demodulation

*accepted ICSPCS, Australia, December 2019



FUTURE EXTENSIONS

- ❖ Target detection **trough wall**
- ❖ Target **localization**

Machine Learning for Wireless Network Topology Inference

Enrico Testi, Elia Favarelli, Lorenzo Pucci, and Andrea Giorgetti
DEI, University of Bologna
Via dell'Università 50, 47522 Cesena, Italy
e-mail: {enrico.testi4, elia.favarelli2, andrea.giorgetti}@unibo.it

Abstract—In this work, we propose a new framework for blind wireless network topology inference and present a novel solution based on machine learning (ML) techniques. In particular, we seek to identify a causal relationship between the patterns of the radio-frequency (RF) transmissions of the nodes in the network from over-the-air signals observed by a cloud of sensors uniformly distributed in the network landscape. The proposed framework is based on simple RF sensors that measure the received power at a rate sufficient to extract traffic patterns. Numerical results based on simulated data show how, despite the propagation impairments and noise may affect the performance of the algorithms, the neural network (NN)-based solution reaches 93% of accuracy even with a relatively low number of sensors.

I. INTRODUCTION

The importance of networks, in their broad sense, is rapidly and massively growing in modern-day society thanks to unprecedented communication capabilities offered by technology. This aspect is even more exacerbated by the upcoming, if not already happening, revolution of cyber-physical systems (CPSs).

In this scenario of ultra-densely connected objects the knowledge of network topology, at different levels of abstractions, is an essential aspect that can help to predict traffic flow, infer the potential receivers of a currently active transmitter, understand the degree of connectivity of users, detect the presence of communities, help network maintenance, optimization, and orchestration. Moreover, in defense applications, understanding the structure of an adversary's network may considerably help to avoid dangerous situations, making predictions, and designing decision-making strategies.

In many of the above-mentioned scenarios, it seems very important, if not mandatory, that network topology is inferred without the need of being a part of it or without increasing the network overhead sharing topology information [1], [2]. For this reason, in the last decade, there has been an increasing interest in the possibility of reconstructing the structure of a network from few observed quantities at some nodes (or at the edges) with little, if not zero, a priori knowledge of the network structure [3], [4]. If the problem appears rather complicated for a wired network, it can be even more challenging in a wireless scenario because of channel impairments, interference, path loss, shadowing and fading, and the so-called hidden terminal problem. In fact, if we consider a

large wireless network, on one side, the potential connection between the nodes could be inferred, for example, based upon the distance between them. On the other side, many nodes can be within communication range of many others and have the potential to communicate with all of them. In this situation, inferring which nodes are actually communicating, basing upon the patterns of their activity, might be very useful.

Focusing on wireless networks, the rapidly growing demand for radio services by billions of devices will make the radio spectrum an increasingly valuable resource. From this perspective, cognitive radio (CR) devices will have to probe the RF scene in time, space and frequency domain to ensure that a well-defined portion of the spectrum is free, making multidimensional spectrum analysis mandatory [5], [6], [7]. In this context, spectrum awareness, for which network topology plays a crucial role, will be of paramount importance.

A. Existing works

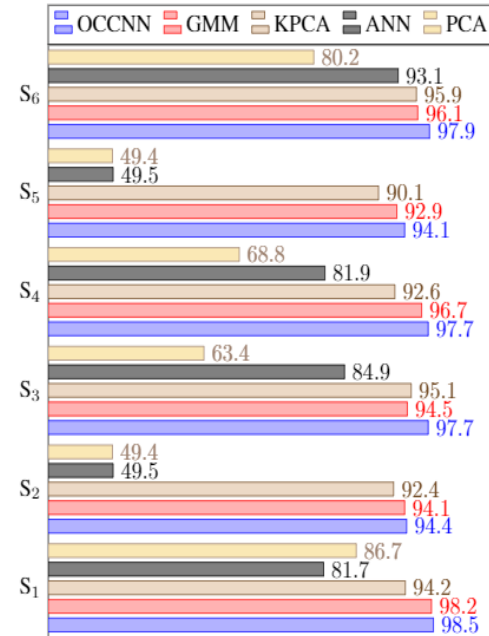
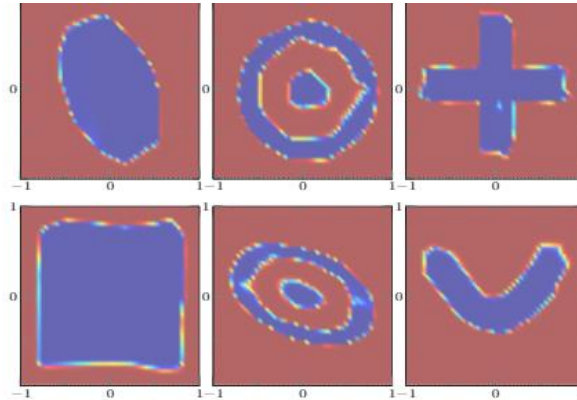
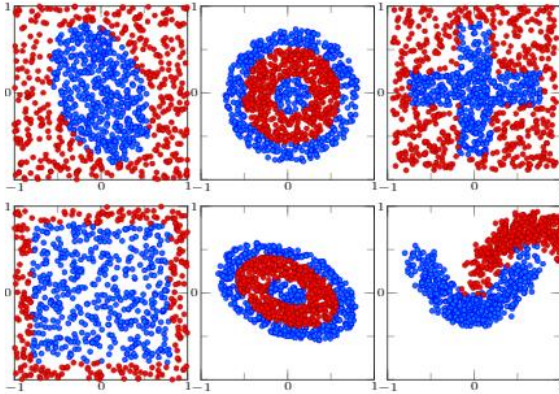
There are different approaches and methodologies for network topology inference proposed in the literature. Some of them, such as [8], exploit spectral coherence as a measure of causality between two signals. Hence, a decision test with a threshold is used to detect causal relations in the traffic generated by the nodes. The main issue of this approach is that it is challenging to choose the correct frequency and the optimal threshold for the decision test. Moreover, solutions of this kind rely upon the notion of correlation which, in principle, does not necessarily imply causation. The task of network topology inference can be seen as learning temporal causal structures among multiple time series. This reminds the well-known causality inference problem described by Pearl [9] and Granger [10]. In particular, Granger auto-regressive (AR) model introduced in [10] for econometric time series analysis has been employed more recently in computational neuroscience and neuroimaging, studying the interactions between neurons in the brain [11], [12]. Granger causality (GC) based techniques allow the identification of a threshold on a parametric statistical test to make a decision [13], [14]. A specific formulation of GC named asymmetric Granger causality (AGC) is exploited in [15], where the parametric tests are carried out over groups of time series as will be explained in Section III. Another approach for causal inference on networks, that is optimum under certain restrictive *Markovian*

- ❖ Network simulation
- ❖ Spatial filtering
- ❖ Excision filtering
- ❖ Wifi protocol
- ❖ Feature extraction
- ❖ Sample mean
- ❖ Sample variance
- ❖ Channel model
- ❖ Granger causality
- ❖ Transfer entropy
- ❖ NN
- ❖ Accuracy
- ❖ NN provide better performance with lower complexity

FUTURE EXTENSION

- ❖ Node localization
- ❖ Blind source separation

*accepted ICSPCS, Australia, December 2019



QUESTION

Why **OCCNN overcome** always the performance of the others algorithms except in the **SHM** scenario?

ANSWER

This happens because the points are **not uniformly distributed** in the feature space hence the **Pollard's** estimator **wrong estimate** density

POSSIBLE SOLUTION

Adopt different techniques to **estimate non-uniform density**

NEW SCENARIOS

- ❖ Investigate the effects of **quantization** on the accelerometers data
- ❖ Study the effects of **sensor failure** on the detection accuracy
- ❖ Proposal of new technique to extract **damage sensitive features**

Thanks for the attention!